Vol. 01 (2025) 141-151, DOI: 10.61552/EC.2025.011

Energy Catalyst

www.jme.aspur.rs

Two Novel Models for Predicting the Transmittance of Dielectric Crossed Compound Parabolic Concentrator (dCCPC) Under Various Sky Conditions

Meng Tian[a,c], Li Zhang[b,c,*], Yuehong Su[c]

[a]*Shenzhen Key Laboratory for Optimizing Design of Built Environment, School of Architecture and Urban Planning, Shenzhen University, Shenzhen, 518060, China,*
[b]*School of Architecture and Design, China University of Mining and Technology, Xuzhou, 221000, China,*
[c]*Department of Architecture and Built Environment, Faculty of Engineering, University of Nottingham, University Park, Nottingham NG7 2RD, UK.*

Keywords:

Dielectric crossed compound parabolic concentrator (dCCPC), Compound parabolic concentrator (CPC), Artificial neural network (ANN), Transmittance

* Corresponding author:

Li Zhang
E-mail: 6610@cumt.edu.cn

Received: 4 September 2025
Revised: 20 October 2025
Accepted: 5 December 2025

A B S T R A C T

The dielectric crossed compound parabolic concentrator (dCCPC) exhibits significant potential for solar energy harvesting in photovoltaic applications and daylighting optimization in architectural design. Transmittance is a fundamental property that assesses the optical performance of dCCPC, which has been determined by ray-tracing simulation traditionally. However, this approach is computationally intensive and constrained by the sky models implemented in optical simulation tools. This study employed both multiple nonlinear regression (MNLR) and artificial neural network (ANN) models to predict dCCPC transmittance under all sky conditions including clear, intermediate and overcast skies. The high agreement of predicting results revealed the feasibility and accuracy of both methods, which achieved a coefficient of determination (R^2) exceeding 0.93 and a mean square error (MSE) below 0.3%. Both methods offer the advantages of simplicity, speed, and accuracy for determining dCCPC's optical performance, while the choice between them should be based on specific practical requirements.

1. INTRODUCTION

With the consideration of raising problems in building design, such as visual comfort, overheating and energy saving, daylighting control has become an essential part in sustainable building practices [1,2]. In a survey conducted by Reinhart and Fitz [3], 91% of 185 interviewees related to architecture and building energy from 27 countries had considered daylighting aspects in their building design.

For decades, the compound parabolic concentrator (CPC) has been a widely employed

nonimaging optical device for solar thermal and electrical applications [4-7]. In recent years, the potential of the CPC in daylighting control has raised attention from researchers. Owing to its unique structure, the CPC can selectively admit or block direct solar radiation and diffuse skylight based on the incident angle of incoming light, thereby enabling effective daylight control.

There are a number of applications of CPC in daylighting. Ulavi et al. [8] put forward a hybrid solar window consisting of transparent 2D CPCs and tubular absorbers. The CPC is coated with a wavelength selective film in order to concentrate the sunlight in infrared range onto absorber and transmit the sunlight in visible range into interior spaces. The annual thermal efficiency of this window ranges between 15-26% in the climate of Minneapolis. Similarly, a hybrid window termed PRIDE (Photovoltaic facades of Reduced costs Incorporating Devices with optically concentrating Elements) was also developed, which integrated 2D asymmetric CPCs with PV cells. After several improvements on PRIDE by many researchers [9-11], the typical type of PRIDE can provide the maximum power output which is 3.27 times as high as a flat PV of the same area [9]. Meanwhile, PRIDE also controls daylighting by its parabolic surfaces.

The dielectric CPC (dCPC) is regarded as a type of CPC which enlarges its acceptance angle due to the refraction on air-dielectric interface [12], so it can receive more sunlight comparing with conventional mirror CPC. As a result, it has become more popular in CPC application, especially in daylighting control. Yu et al. [13] investigated the feasibility of a 2D dCPC in daylighting control when it is used as skylights for atrium. It was found that the transmittance provided by dCPC is lower in summer and higher in winter, which can prevent overheating in the summer effectively. The transmittance is relatively high under overcast sky condition so that the indoor illuminance level can be maintained. Tian and Su [14] investigated the potential of three-dimensional (3D) dCCPC on daylighting control. Comparing with 2D dCPC, it presents better capability on controlling daylight not only in different seasons during a whole year, but in different times through a whole day. For example, during the summer solstice, the transmittance of 3D dCCPC reaches approximately 0.8 in both the morning and afternoon, whereas it decreases to around 0.4 at noon. On the contrary, on the winter solstice, the transmittance measures about 0.4 in the morning and rises to 0.6 by midday. Tian et al. [15] evaluate the energy saving potential of using a miniature dCCPC as skylights in buildings, and find that the annual energy saving can reach 13% in locations with long hot seasons.

As more and more studies have been conducted to investigate the feasibility of CPC in daylighting control, an accurate and reliable model for calculating or predicting the transmittance of CPC becomes significant. The optical efficiency of CPCs is typically assessed through ray-tracing software, for instance, Matlab [16], LightTools [17], Radiance [18], Photopia [19], and COMSOL Multiphysics [20], etc. They combine the advantages of illuminance calculation and interior visualization. Many studies have proved the reliability and accuracy of raytracing simulations [21-23]. However, raytracing simulation takes a long time for complex light path and is impracticable for a performance analysis on an annual basis. Except simulation, few of researches have brought forward simple, fast and accurate mathematical models or other approaches to predict CPC performance, especially for dCPC which has complex light reactions including reflection, refraction and total internal reflection.

To characterize the optical perfromance of 2D dCPCs, Yu and Su [24] proposed a concept 'inner projection angle' to represent the refracted angle that incident light assumes within the device. By evaluating the performance of these structures under various incident angles, their research revealed strong correlations for the dCPCs with base coating: between this inner projection angle and optical efficiency, as well as between the angle and the combined magnitude of transmittance and surface reflection. As regards 3D dCPC, our previous work [25] derived new mathematical models to predict the transmittance and optical performance of dCCPC under clear sky condition.

Artificial neural network (ANN), usually called neural network, is an alternative to traditional simulation method, which is a self-learning and self-training programme. A neural network can

be considered as a network of neurons which interact with each other in a specific order through mathematical functions. It has been widely applied to various disciplines, such as renewable energy, heat exchange, refrigeration, chemical process control, and building design, etc., for data analysis and prediction [26-28].

ANN has also been used as a powerful forecasting tool in aspect of daylighting including luminance value, daylighting performance, energy saving for building and daylighting control system [29-32]. Navada et al. [33] attempted to predict outdoor and indoor illuminance level through ANN in order to control the position of blinds, and the predicted results matched the experiment values very well. Kandasamy et al. [34] developed a smart lighting control system using ANN and internal model control (IMC) to achieve personalized lighting levels for occupants while simultaneously harvesting daylight to reduce energy consumption. Seyedolhosseini et al. [35] proposed a daylight-adaptive and energy-efficient smart indoor lighting control method based on ANN, which achieved an average mean square error of 1.2 between desired and measured illuminance, indicating high accuracy.

Based on our previous work [25], this study extends the MNLR model for predicting the transmittance of 3D dCCPC to accommodate all standard sky conditions, using solar azimuth, solar altitude and sky clearness as inputs. Additionally, an ANN model was developed to forecast dCCPC transmittance. The accuracy, feasibility, advantages and limitations of both models are compared and discussed.

2. METHODOLOGY

2.1 Model description

In this study, we compare two types of dCCPCs. The first is the conventional, non-coated dCCPC, characterized by its fully transparent construction from a material like acrylic. The second is a modified version where the device's base is equipped with a black, light-absorbing surface intended to minimize loss due to reflection. The dCCPC attached with a PV cell on its base is considered as base-coated dCCPC in most cases. Fig. 1 illustrates the dimensions of the sample dCCPC used in this study, which consist of four parabolic surfaces and two square apertures. The performance of dCCPC is simulated by PHOTOPIA, which is a professional and precise optical analysis tool [19]. Three standard sky models, clear sky, intermediate sky and overcast sky, are used to cover all typical sky conditions. All sky models are based on the equations defined in CIE standard [36] and IES RP-21 [37].

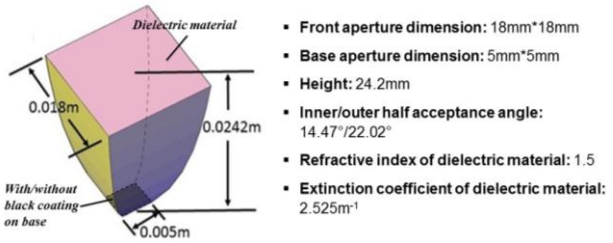

Fig. 1. Schematic and dimensions of dCCPC.

Similar to the previous study [25], the independent variables for prediction models are solar altitude (θ_h), solar azimuth (γ), and sky clearness factor (ε). For the input data set, the solar altitude ranges from 10° to 90°, and the solar azimuth ranges from 0° to 45° considering the symmetry of dCCPC. The sky clearness factor is equal or greater than 1. According to the sky model proposed by Perez, et al. [38], when $1 \leq \varepsilon \leq 1.2$, it refers to overcast sky; $\varepsilon \approx 1.2 \sim 2$ represents overcast to intermediate sky; $\varepsilon \approx 2 \sim 3$ indicates intermediate to clear sky; when $\varepsilon > 3$, it implies clear sky. The sky clearness factor is defined by Eq. 1 [39] in detail.

$$\varepsilon = \frac{\frac{(I_h + I)}{I_h} + kZ^3}{1 + kZ^3} \quad (1)$$

where I is direct normal solar irradiance; I_h is diffuse horizontal irradiance; k is a constant and equals 1.041 for solar zenith angle Z in radians.

The dependent variable of the prediction model is the transmittance (T) of dCCPC, which quantifies the proportion of incident light successfully transmitted through the device, as shown in Eq. 2.

$$T = \frac{E}{E_0} \quad (2)$$

where E is the transmitted daylight illuminance. E_0 is the illuminance received by the entry aperture of dCCPC. T is the transmittance of dCCPC.

2.2 Multiple nonlinear regression (MNLR)

In respect of data-based prediction, the traditional way is to use statistical models. Multiple nonlinear regression (MNLR) is probably the most common approach for dealing with nonlinear relationships with several variables. It is assumed that the relationship between the dependent variable $\boldsymbol{y}$ and the $\boldsymbol{p}$ vector of regressors $\boldsymbol{x_i}$ is nonlinear in MNLR models. The MNLR models for predicting the dCCPC performance were developed by XLSTAT which is an accurate statistical add-in integrated into Microsoft Excel.

The input variables were used to train and test the MNLR models are: solar altitude (θ_h), solar azimuth (γ), and sky clearness factor (ε). According to the previous study [25], the best NMLR model for predicting the dCCPC transmittance under clear sky is as shown by Eq. 3 below:

$$T = a_1 \cos(b_1\theta_h + b_2) \cdot \cos(b_3\gamma + b_4) \cdot \left(c_1 + c_2\varepsilon + c_3\gamma + c_4\theta_h + c_5\theta_h\gamma + c_6\varepsilon\gamma + c_7\theta_h\varepsilon + c_8\varepsilon^2\theta_h\gamma + c_9\theta_h^2\varepsilon\gamma + c_{10}\gamma^2\varepsilon\theta_h + c_{11}\varepsilon^2\theta_h^2\gamma^2 + c_{12}\varepsilon^2 + c_{13}\theta_h^2 + c_{14}\gamma^2\right) + a_2 \quad (3)$$

Where θ_h is altitude (expressed in radian measure); γ is azimuth (expressed in radian measure); ε is sky clearness factor; T is transmittance; a_n, b_n, c_n are regression coefficients.

2.3 Artificial Neural Network (ANN)

Artificial Neural Network (ANN) is an alternative way to extract the nonlinear relationships between the variables by self-training and self-learning through black-box modelling [40]. It is good at solving multi-variable problems and extracting the non-linear relationship by means of training data.

The multi-layer perceptron (MLP) is the most commonly used neural network, in which every neuron organized in different layers interacts with the neurons in contiguous layers. A typical feedforward artificial neural network consists of three layers of neurons which are input layer, hidden layer and output layer. The input layer contains all of the input parameters, and then they are processed through the network in a forward direction, layer by layer until the output information is computed by the output layer.

Fig. 2 demonstrates the ANN frame utilized in this study. The ANN model is composed of an input layer with two or three input parameters depending on different models, a hidden layer, and an output layer containing one output parameter. The mathematical form of this three-layer feedforward ANN is expressed as Eq. 4 [41].

$$O = g_2\left[\sum_j Z_j v_j \, g_1\left(\sum_i w_{ji} I_i + w_{j0}\right) + v_0\right] \quad (4)$$

where I_i is the value of node i in the input layer; Z_j is the value of node j in the hidden layer; O is the value output from the node in the output layer; w_{j0} are the weights of bias input node $I_0 = 1$ and v_0 is the weight of bias input from hidden unit $Z_0 = 1$; w_{ji} is the weight going to hidden node j from input node i, and v_j is the weight connecting hidden node j to the output node; g_1 and g_2 are the transfer functions for the hidden layer and the output layer.

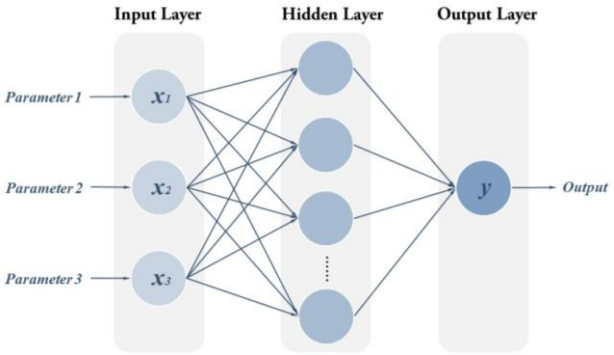

Fig. 2. Feedforward ANN architecture with one hidden layer.

The training algorithm applied in this study for ANN model is Levenberg-Marquardt (LM) by which the weight and bias values are updated. The LM algorithm is an optimization of the Newton algorithm which improves second-order training speed without computing the exact Hessian matrix, and provides stable and fast convergence [42]. Many studies have demonstrated the advantages of the LM algorithm comparing with other training algorithms [43-45]. The LM algorithm is defined by Eq. 5 [46].

$$X_{k+1} = X_k - [J^T J + \mu I]^{-1} J^T \mathrm{e} \quad (5)$$

where X is the criteria of the neural network that would be optimized; J is the Jacobian matrix that contains first derivatives of the network errors in terms of weight and bias; e is the vector of all error terms; μ is the combination coefficient controlling the learning process; I is the identity matrix.

The Neural Network Toolbox in MATLAB 2016b was chosen to build ANN model in this study. All of the ANN models utilize Levenberg-Marquardt back propagation (BP) training algorithms due to its reliability and simplicity [47]. In each ANN model, the total 1050 dataset are randomly divided into three parts: 70% of them was used for training, 15% for validation and 15% for testing. The number of neurons in the hidden layer is optimized based on the available data through the trial-and-error procedure. It was found that the hidden layer with 20 neurons would result in the best performance for the ANN models used in this study. Tansig and purelin functions are selected as the first and second transfer functions after various attempts, which can lead to the best results. Similarly, the input variables are solar altitude (θ_h), solar azimuth (γ), and sky clearness factor (ε), and the output variable is transmittance (T).

2.4 Evaluation criteria

To evaluate regression quality, we employ the coefficient of determination (R^2), sum of squared errors (SSE) and mean squared error (MSE), defined respectively in Eqs 6, 7 and 8.

$$R = \frac{n\sum y_i\hat{y}_i - (\sum y_i)(\sum \hat{y}_i)}{\sqrt{n(\sum y_i^2) - (\sum y_i)^2}\sqrt{n(\sum \hat{y}_i^2) - (\sum \hat{y}_i)^2}} \quad (6)$$

where R is correlation coefficient; R^2 is coefficient of determination; $\hat{y}_i$ is the value of the dependent variable predicted by the model; y_i is the true value of the dependent variable; n is the number of samples.

$$SSE = \sum_{i=1}^{n}(y_i - \hat{y}_i)^2 \quad (7)$$

where SSE is the sum of squared errors of prediction.

$$MSE = \frac{SSE}{n} \quad (8)$$

Each of the criteria refers to a specific property of regression data. Typically, higher R^2 (closer to 1) indicates greater predictive accuracy, while MSE <10% signifies high precision [48].

3. MODIFICATION OF MULTIPLE NONLINEAR REGRESSION (MNLR) MODEL

It is known that dCCPC accepts light with larger incident angle, and rejects light with smaller incident angle. For a sky, the incident light consists of direct light from the sun and diffuse light from the sky. The optical performance of dCCPC—encompassing transmittance and efficiency—exhibits significant angular sensitivity to direct solar irradiance. Thus, transmittance varies most significantly under clear skies, varies moderately under partially cloudy conditions, and remains relatively stable under overcast skies [49,50]. Therefore, a modified mathematical model (Eq. 9a and Eq. 9b) was proposed on the basis of previous work [25] aiming at determining the transmittance of both non-coated and base-coated dCCPC under all standard sky conditions: Eq. 9a is suitable for the clear and intermediate skies and Eq. 9b is for overcast condition.

$$T(\theta_h, \gamma, \varepsilon) = \begin{cases} a_1 \cos(b_1\theta_h + b_2)\cos(b_3\gamma + b_4)(c_1 + c_2\varepsilon + c_3\gamma + c_4\theta_h \\ +c_5\theta_h\gamma + c_6\varepsilon\gamma + c_7\theta_h\varepsilon + c_8\varepsilon^2\theta_h\gamma + c_9\theta_h^2\varepsilon\gamma + c_{10}\gamma^2\varepsilon\theta_h, & \varepsilon > 1.2 \quad (9a) \\ +c_{11}\varepsilon^2\theta_h^2\gamma^2 + c_{12}\varepsilon^2 + c_{13}\theta_h^2 + c_{14}\gamma^2) + a_2 \\ \\ T_0, & 1 \le \varepsilon \le 1.2 \quad (9b) \end{cases}$$

where θ_h is altitude in radians, $0° < \theta_h \le 90°$; γ is azimuth in radians, $0° \le \gamma \le 45°$, and $\gamma = 0°$ for light projection normal to the entry aperture's side; ε is sky clearness; T is transmittance; a_n, b_n and c_n are regression coefficients; T_0 is the transmittance of dCCPC under overcast sky.

The simulation results of dCCPC transmittance under clear sky, intermediate sky and overcast sky are applied to the regression of Eq. 9a-9b. The values of parameters are illustrated in Table 1 for base-coated and non-coated dCCPC respectively. According to our previous research [25], the regression of base-coated dCCPC is divided into two parts by altitude in order to get better regression results. Fig. 3 and Fig. 4 compares the simulated values with the predicted values generated by Eq. 9a. Because the transmittance of dCCPC is regarded as constant under overcast condition, that is when $1 \le \varepsilon \le 1.2$, Eq. 9b is excluded in comparison.

Table 1. Parameter values of Eq. 9a-9b for different dCCPCs.

Non-coated dCCPC					
a_1	1.92522	c_2	0.01374	c_9	-0.00474
a_2	0.56370	c_3	-0.45392	c_{10}	0.01027
b_1	1.80728	c_4	-0.00785	c_{11}	-0.00026
b_2	1.36934	c_5	0.48689	c_{12}	-0.00014
b_3	2.01738	c_6	-0.02002	c_{13}	-0.21601
b_4	2.31492	c_7	-0.00734	c_{14}	-0.23176
c_1	0.30229	c_8	0.00058	T_0	0.63267
Base-coated dCCPC (θ_h<70°)					
a_1	1.51451	c_2	0.02316	c_9	0.01683
a_2	0.17648	c_3	-0.66508	c_{10}	-0.04433
b_1	1.09774	c_4	-0.53359	c_{11}	-0.00057
b_2	2.18317	c_5	-0.23800	c_{12}	-0.00058
b_3	2.19941	c_6	0.00115	c_{13}	0.16767
b_4	1.79765	c_7	-0.03045	c_{14}	0.65415
c_1	0.79983	c_8	0.00191	T_0	0.52864
Base-coated dCCPC (θ_h>70°)					
a_1	8.24190	c_2	0.00530	c_9	-0.00587
a_2	0.33604	c_3	-0.01065	c_{10}	-0.00129
b_1	0.18880	c_4	0.08257	c_{11}	0.00012
b_2	4.32194	c_5	-0.05855	c_{12}	-0.00006
b_3	4.88711	c_6	-0.00045	c_{13}	0.00010
b_4	-0.72973	c_7	0.02421	c_{14}	0.04963
c_1	-0.05998	c_8	-0.00036	T_0	0.52864

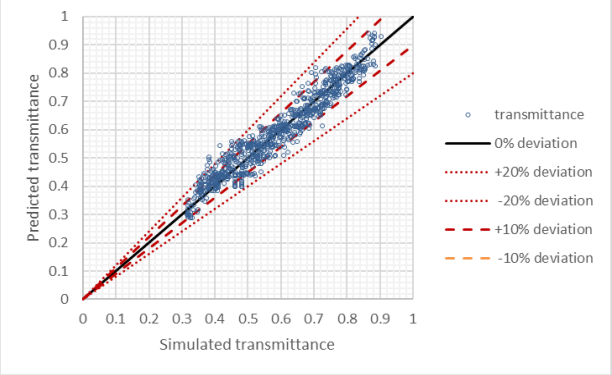

Fig. 3. Comparison between simulated and predicted results of non-coated dCCPC under clear and intermediate skies (MNLR, Eq. 9a).

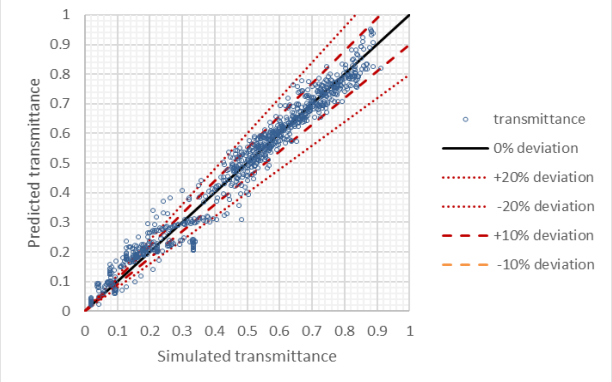

Fig. 4. Comparison between simulated and predicted results of base-coated dCCPC (MNLR, Eq. 9a).

It can be seen that the regression of Eq. 9a provides very strong fittings for non-coated dCCPC. The coefficient of determination (R^2) reaches 0.93 and the MSE is 0.0016. More than 82.5% of the residuals deviations are within ±10%, and 98.5% of the deviations are within ±20%. The goodness of regression for base-coated dCCPC seems not as good as the non-coated one, but still a satisfactory result. It offers a higher R^2 of 0.97 and a relatively lower MSE of 0.0030 which proves its reliability and accuracy. The percentage of the deviations of residuals that is within ±20% is 80.1%. In addition, most of the large deviations occur when the transmittance is smaller than 0.35, because the smaller reference values cause larger percent deviations for the same residuals.

4. DEVELOPMENT OF ARTIFICIAL NEURAL NETWORK (ANN) MODEL

We also developed ANN models to predict the optical performance of dCCPC. As ANN is a data-driven process built upon a flexible mathematical algorithm, all models were trained, tested and validated using the consistent combinations of dependent and independent variables, as used in the regression analysis. For all input data in each ANN model, 70% was randomly selected to be used for training, 15% was for test and the rest of 15% was for validation.

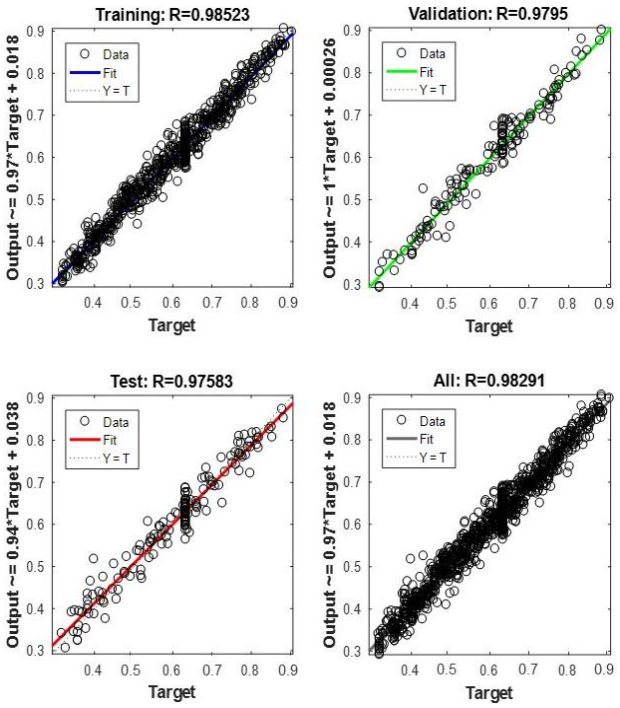

Fig. 5. Comparison between predicted values and simulation values (target) obtained in training, validation and test processes of ANN (Independent variables: θ_h, γ, ε; Dependent variable: T for non-coated dCCPC).

Fig. 5 demonstrates an example of the ANN model results that predict the transmittance (T) of non-coated dCCPC. The data used for training each ANN model include all the three sky types: clear sky, intermediate sky and overcast sky. For verifying and comparing with regression results, the results of all data (100%) obtained from ANN models would be processed and applied in this section.

Table 2 summarizes the correlation coefficients (R) and mean square errors (MSE) of ANN models aiming at the combinations of independent and dependent variables of obtained regression equations. It can be found that all of the correlation coefficients are higher than 0.99 and MSEs are less than or equal to 0.0006, which mean the ANN models provide reliable predictions that are very close to input values. The results of each model would be discussed in details in the following parts.

Table 2. Correlation coefficients of trained ANN models.

CPC type	Independent variables	Dependent variables	R				MSE
			Training (70%)	Validation (15%)	Test (15%)	All (100%)	
Non-coated	$\theta_h, \gamma, \varepsilon$	T	0.9852	0.9795	0.9758	0.9829	0.0006
Base-coated	$\theta_h, \gamma, \varepsilon$	T	0.9936	0.9905	0.9906	0.9927	0.0007

The simulated and ANN-predicted results of transmittance for non-coated dCCPC are shown in Fig. 6. Comparing with the predicted results gained from regression demonstrated in Fig. 3, it can be seen that more results, up to 96%, are located within the regions of ±10% deviations. The R^2 reaches 0.966 which is higher than that of regression. Similar to the ANN predictions for non-coated dCCPC, the ANN prediction model is slightly better than the MNLR model for base-coated dCCPC with the R^2 of 0.986. Over 86% of the predicted values fall within a ±20% deviation margin as shown in Fig. 7. Compared to the regression results in Fig. 4, it is interesting to see that the deviations of these two models have something in common: relatively large deviations occur when the transmittance is less than 0.5. Results reveal that ANN is a relatively accurate and reliable approach to predict the transmittance of non-coated dCCPC with inputs of altitude, azimuth and sky clearness. Moreover, although the deviations of ANN model are smaller than that of regression model generally, the tendencies or error occur of both regression and ANN models are the same.

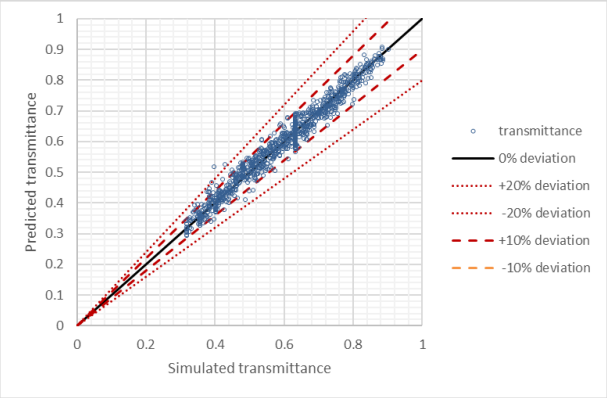

Fig. 6. Comparison of predicted and simulated results of non-coated dCCPC (ANN)

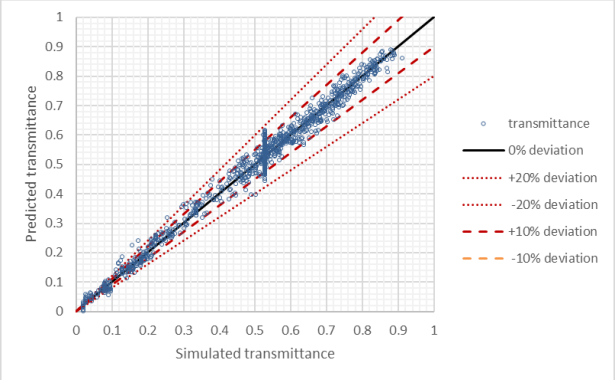

Fig. 7. Comparison of predicted and simulated results of base-coated dCCPC (ANN)

5. ADVANTAGES AND LIMITATIONS

5.1 Comparison between ANN and regression

The results obtained from the best regression and ANN models for different CPC types are illustrated in Table 3 below. All models demonstrate an R^2 exceeding 0.93. Although ANN and MNLR models are capable of accurately predicting the nonlinear relationship, the ANN model consistently demonstrates slightly higher accuracy.

Both of ANN and regression are fast and feasible methods for data prediction, but they have their own specific advantages and drawbacks. ANN is a data-driven process based on flexible algorithms and it can provide more precise forecast as a result of its specific neural network. Its main drawback is black-box modelling, which means it cannot provide available formula or visualized calculation procedures. On the contrary, regression model gives a specific formula which demonstrates the relationships among variables clearly.

Table 3. Comparison between the correlations of regression formula and ANN model

CPC type	Independent variables	Dependent variables	Regression		ANN	
			R^2	MSE	R^2	MSE
Non-coated	$\theta_h, \gamma, \varepsilon$	T	0.931	0.0016	0.966	0.0006
Base-coated	$\theta_h, \gamma, \varepsilon$	T	0.969	0.0030	0.986	0.0007

It is easy for people to understand and formula is more likely to be accepted when cooperating with other software. In addition, dCCPC is designed for controlling daylight for the purpose of saving energy for building. Many software related to building energy simulation are capable to cooperate with customized input formula for specific devices, while not that many platforms support the ANN program. In aspect of the improvement and simplification of models, ANN is more flexible than MNLR models. MNLR model is good at dealing with the variables having obvious and regular relationships, like the relationships among sky clearness factor, sun position and transmittance referred to in this study. ANN is not limited in specific criteria and can build prediction model for the variables without obvious correlations. Many studies [19,51,52] have attempted to forecast the daylight such as sky illuminance or luminous efficacy through ANN successfully, which implies it is highly possible to build the ANN model to predict the dCCPC performance with other input variables relating to sun and sky, for example, solar radiation, direct sunlight illuminance, and global horizontal illuminance, etc. The advantages and drawbacks of MNLR and ANN models are summarized in Fig. 8. Both of the ANN and regression present promising results in predicting optical performance of dCCPC, the selection of these two methods should be determined by the requirements under different conditions.

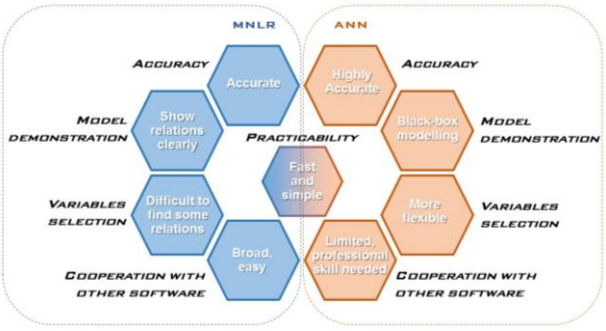

Fig. 8. Summary of pros and cons for MNLR and ANN models.

5.2 Significance and limitation of prediction models

Two transmittance prediction approaches were evaluated and compared for both base-coated and non-coated dCCPCs, utilizing simulation data from the precision optical tool PHOTOPIA. The dataset consists of the transmittance across three typical sky conditions—clear, intermediate and overcast—according to the standard sky models defined by the CIE Standard [36] and IES RP-21 [37]. However, the actual sky changes all the time leading to various luminance distribution, i.e. 15 sky types are proposed in CIE Standard in total. Also, considering the errors of these empirical sky models, small errors may occur when using prediction models in practice. However, this can be improved by using data obtained from actual conditions as input. In this study, both MNLR and ANN models are data-driven models, which means the basic input data set are required when building the prediction models. Generally speaking, the more referenced data is input, the more accurate the forecasting models will be. The input data could be simulation or experiment data.

Based on the proposed prediction models, the transmittance of dCCPC under arbitrary sky conditions can be determined rapidly with the known of local sun position, dCCPC orientation and sky clearness factor, which saves the time on optical simulations. The energy saving on building from dCCPC can also be calculated under the cooperation with software simulating the energy consumption of building. On the other hand, the MNLR and ANN models put forward are not appropriate for not only the specific dCCPC used in this study, but for the dCCPCs with different dimensions. On account of the similar structures and working principles of all CPCs, like dCCPC, 2D CPC, and mirror CPC, etc., both the two types of prediction models have great potential to be applied for other types of CPC. Finally, as discussed before about the advantages of ANN, it is highly probable that the input variables could be more simple and straightforward, e.g. sky illuminance and direct radiation, etc., to determine the transmittance of dCCPC through ANN.

6. CONCLUSION

This study put forward the MNLR and ANN models for predicting the transmittance of both base-coated and non-coated dCCPC based on numerous simulation results. These models encompassed all standard sky scenarios, such as overcast, intermediate, and clear skies. Three key parameters, which were solar altitude, solar azimuth and sky clearness factor were selected as the independent variables. The R^2 values are higher than 0.93 for the MNLR models and higher than 0.96 for the ANN models. Most of the predicted values deviated by less than 20% when compared to the input data.

The results indicate that both the MNLR and ANN models are accurate and reliable for determining dCCPC transmittance. The two models have their specific advantages and drawbacks. ANN models provide slightly better results than MNLR models owing to its special mechanism of network. Regression models present clear relationships among variables while ANN is black-box modelling process. MNLR models are easier to incorporate with other software but ANN models are more powerful when building complex and irregular relations among variables. Therefore, it is suggested to choose different models depending on the requirements and the features of these two methods. The proposed frameworks exhibit considerable potential for practical use: they significantly reduce the time required for ray-tracing simulations and can be adapted to various dCCPC types. Furthermore, these models show promise for predicting the optical performance of other CPC types under real sky conditions. Future work may focus on identifying more straightforward input variables to further simplify model structures and enhance computational efficiency.

Acknowledgement

We would also like to thank Dr Mark Jongewaard from Photopia for creating intermediate sky models for this study.

REFERENCES

[1] A. Kangazian and S. Z. Emadian Razavi, “Multi-criteria evaluation of daylight control systems of office buildings considering daylighting, glare and energy consumption,” *Sol. Energy*, vol. 263, p. 111928, 2023.

[2] M. Hazbei, N. Rafati, N. Kharma, and U. Eicker, “Optimizing architectural multi-dimensional forms; a hybrid approach integrating approximate evolutionary search, clustering and local optimization,” *Energy Buildings*, vol. 318, p. 114460, 2024.

[3] C. Reinhart and A. Fitz, “Findings from a survey on the current use of daylight simulations in building design,” *Energy Buildings*, vol. 38, pp. 824–835, 2006.

[4] Y. Dan, M. Hu, Q. Wang, Y. Su, and S. Riffat, “Comprehensive evaluation of integrating radiative sky cooling with compound parabolic concentrator for cooling flux amplifying,” *Energy*, vol. 312, p. 133673, 2024.

[5] F. Masood et al., “The compound parabolic concentrators for solar photovoltaic applications: Opportunities and challenges,” *Energy Rep.*, vol. 8, pp. 13558–13584, 2022.

[6] C. Jiang, L. Yu, S. Yang, K. Li, J. Wang, P. D. Lund, and Y. Zhang, “A Review of the Compound Parabolic Concentrator (CPC) with a Tubular Absorber,” *Energies,* vol. 13, p. 695, 2020.

[7] D. Kumar et al., “Design and development of a novel and cost effective modified Compound parabolic trough collector,” *Energy Convers. Manag.*, vol. 306, p. 118285, 2024.

[8] T. Ulavi, T. Hebrink, and J. H. Davidson, “Analysis of a hybrid solar window for building integration,” *Sol. Energy*, vol. 105, pp. 290–302, 2014.

[9] N. Sarmah and T. K. Mallick, “Design, fabrication and outdoor performance analysis of a low concentrating photovoltaic system,” *Sol. Energy*, vol. 112, pp. 361–372, 2015.

[10] [10] N. Sarmah, B. S. Richards, and T. K. Mallick, “Design, development and indoor performance analysis of a low concentrating dielectric photovoltaic module,” *Sol. Energy*, vol. 103, pp. 390–401, 2014.

[11] H. Baig, N. Sarmaah, D. Chemisana, J. Rosell, and T. K. Mallick, “Enhancing performance of a linear dielectric based concentrating photovoltaic system using a reflective film along the edge,” *Energy*, vol. 73, pp. 177–191, 2014.

[12] W. T. Welford and R. Winston, *The Optics of Nonimaging Concentrators: Light and Solar Energy*. New York, NY, USA: Academic Press, 1978.

[13] X. Yu, Y. Su, H. Zheng, and S. Riffat, "A study on use of miniature dielectric compound parabolic concentrator (dCPC) for daylighting control application," *Build. Environ.*, vol. 74, pp. 75–85, 2014.

[14] M. Tian and Y. Su, "A study on use of three-dimensional miniature dielectric compound parabolic concentrator (3D dCPC) for daylighting control application," in *Proc. 14th Int. Conf. Sustain. Energy Technol. (SET 2015)*, Nottingham, UK, 2015.

[15] M. Tian, L. Zhang, Y. Su, Q. Xuan, G. Li, and H. Lv, "An evaluation study of miniature dielectric crossed compound parabolic concentrator (dCCPC) panel as skylights in building energy simulation," *Sol. Energy*, vol. 179, pp. 264–278, 2019.

[16] MathWorks, *MATLAB*. [Online]. Available: http://uk.mathworks.com/index.html?s_tid=gn_logo. Accessed: Feb. 13, 2016.

[17] Synopsys, *LightTools Illumination Design Software*. [Online]. Available: https://optics.synopsys.com/lighttools/lighttools-product-literature.html. Accessed: Feb. 13, 2025.

[18] Lawrence Berkeley National Laboratory, *Radiance*. [Online]. Available: http://radsite.lbl.gov/radiance/framew.html. Accessed: Feb. 15, 2025.

[19] *Photopia User's Guide*. [Online]. Available: http://www.ltioptics.com/en/photopia-standalone-base.html. Accessed: Apr. 5, 2025.

[20] COMSOL AB, *Introduction to COMSOL Multiphysics*. [Online]. Available: https://www.comsol.com/comsol-multiphysics#overview. Accessed: Feb. 15, 2016.

[21] Q. Xuan et al., "Analysis and quantification of effects of the diffuse solar irradiance on the daylighting performance of the concentrating photovoltaic/daylighting system," *Build. Environ.*, vol. 193, p. 107654, 2021.

[22] S. A. Waghmare and N. P. Gulhane, "Design configurations and possibilities of reflector shape for solar compound parabolic collector by ray tracing simulation," *Optik*, vol. 176, pp. 315–323, 2019.

[23] S. Foster et al., "Assessment of the RACPC Performance under Diffuse Radiation for Use in BIPV System," *Appl. Sci.*, vol. 10, 2020.

[24] X. Yu and Y. Su, "A discussion of inner south projection angle for performance analysis of dielectric compound parabolic concentrator," *Sol. Energy*, vol. 113, pp. 101–113, 2015.

[25] M. Tian and Y. Su, "Multiple nonlinear regression model for predicting the optical performances of dielectric crossed compound parabolic concentrator (dCCPC)," *Sol. Energy*, vol. 160, pp. 310–321, 2018.

[26] W. Cao and C. Zhang, "An effective Parallel Integrated Neural Network System for industrial data prediction," *Appl. Soft Comput.*, vol. 107, p. 107397, 2021.

[27] B. Roter, N. Ninkovic, and S. V. Dordevic, "Clustering superconductors using unsupervised machine learning," *Physica C: Supercond. Appl.*, vol. 598, p. 1354078, 2022.

[28] R. Kumar, R. K. Aggarwal, and J. D. Sharma, "Comparison of regression and artificial neural network models for estimation of global solar radiations," *Renew. Sustain. Energy Rev.*, vol. 52, pp. 1294–1299, 2015.

[29] W. Kim, Y. Jeon, and Y. Kim, "Simulation-based optimization of an integrated daylighting and HVAC system using the design of experiments method," *Appl. Energy*, vol. 162, pp. 666–674, 2016.

[30] Y. Lei et al., "Precise lighting control via automated shading and artificial lighting: A systematic review," *Build. Environ.*, vol. 285, p. 113607, 2025.

[31] F. Kotarela, A. Kyritsis, R. Agathokleous, and N. Papanikolaou, "On the exploitation of dynamic simulations for the design of buildings energy systems," *Energy*, vol. 271, p. 127002, 2023.

[32] J. Ngarambe, I. Adilkhanova, B. Uwiragiye, and G. Y. Yun, "A review on the current usage of machine learning tools for daylighting design and control," *Build. Environ.*, vol. 223, p. 109507, 2022.

[33] S. G. Navada, C. S. Adiga, and S. G. Kimi, "Prediction of Daylight Availability for visual comfort," *Int. J. Appl. Eng. Res.*, vol. 11, pp. 4711–4717, 2016.

[34] N. K. Kandasamy, G. Karunagaran, C. Spanos, K. J. Tseng, and B.-H. Soong, "Smart lighting system using ANN-IMC for personalized lighting control and daylight harvesting," *Build. Environ.*, vol. 139, pp. 170–180, 2018.

[35] A. Seyedolhosseini, N. Masoumi, M. Modarressi, and N. Karimian, "Daylight adaptive smart indoor lighting control method using artificial neural networks," *J. Build. Eng.*, vol. 29, p. 101141, 2020.

[36] British Standards Institution, "Spatial distribution of daylight – CIE standard general sky," *BS ISO 15469:2004*, 2004.

[37] Illuminating Engineering Society of North America, *Calculation of Daylight Availability (IES RP-21)*. New York: IES, 1984.

[38] R. Perez, P. Ineichen, R. Seals, J. Michalsky, and R. Stewart, "Modeling daylight availability and irradiance components from direct and global irradiance," *Sol. Energy*, vol. 44, pp. 271–289, 1990.

[39] *EnergyPlus Version 8.7 Documentation – Engineering Reference*, U.S. Department of Energy, 2016.

[40] I. Lou and Y. Zhao, "Sludge bulking prediction using principle component regression and artificial neural network," *Math. Probl. Eng.*, vol. 2012, p. 17, 2012.

[41] J. Adamowski, H. F. Chan, S. O. Prasher, B. Ozga-Zielinski, and A. Sliusarieva, "Comparison of multiple linear and nonlinear regression, autoregressive integrated moving average, artificial neural network, and wavelet artificial neural network methods for urban water demand forecasting in Montreal, Canada," *Water Resour. Res.*, vol. 48, no. 1, 2012, Art. no. WR011913.

[42] H. Shahzad, M. N. Sadiq, Z. Li, S. Algharni, T. Alqahtani, and K. Irshad, "Scientific computing of radiative heat transfer with thermal slip effects near stagnation point by artificial neural network," *Case Stud. Therm. Eng.*, vol. 54, p. 104024, 2024.

[43] H. E. Abdellatif, S. A. Khan, A. Belaadi, and D. Ghernaout, "Enhancing thermal energy storage: The impact of inclined enclosure geometry and artificial neural network based modeling on phase change material melting performance," *J. Energy Storage*, vol. 114, p. 115750, 2025.

[44] H. Kumar C and R. P. Swamy, "Fatigue life prediction of glass fiber reinforced epoxy composites using artificial neural networks," *Compos. Commun.*, vol. 26, p. 100812, 2021.

[45] T. G. H. Tipu, F. Yao, and T. Anwar, "Bifurcation, chaos, and soliton dynamics in the integrable space curve model: A hybrid analytical and artificial neural network approach," *Chaos Solitons Fractals*, vol. 200, p. 117149, 2025.

[46] MathWorks, *Neural Network Toolbox (R2017a)*. [Online]. Available: https://cn.mathworks.com/help/nnet/index.html. Accessed: Jul. 6, 2025.

[47] S. Haykin, *Neural Networks: A Comprehensive Foundation*. Upper Saddle River, NJ, USA: Prentice Hall PTR, 1998.

[48] C. D. Lewis, *Industrial and Business Forecasting Methods: A Practical Guide to Exponential Smoothing and Curve Fitting*. London, U.K.: Butterworth Scientific, 1982.

[49] A. Rabl, J. O'Gallagher, and R. Winston, "Design and test of non-evacuated solar collectors with compound parabolic concentrators," *Sol. Energy*, vol. 25, no. 4, pp. 335–351, 1980.

[50] Y. Su, S. B. Riffat, and G. Pei, "Comparative study on annual solar energy collection of a novel lens-walled compound parabolic concentrator (lens-walled CPC)," *Sustain. Cities Soc.*, vol. 4, pp. 35–40, 2012.

[51] L. Le-Thanh, H. Nguyen-Thi-Viet, J. Lee, and H. Nguyen-Xuan, "Machine learning-based real-time daylight analysis in buildings," *J. Build. Eng.*, vol. 52, p. 104374, 2022.

[52] T.-L. Le, H. Nguyen-Xuan, and S.-A. Kim, "Hand drawing-based daylight analysis using deep learning and augmented reality," *Results Eng.*, vol. 22, p. 102119, 2024.